# Mechanically tunable metasurface with large gamut of color: Lateral hybrid system Ⓕ

Rui Fang, ⓘD Amir Ghasemi, ⓘD Dagou A. Zeze, et al.

**COLLECTIONS**

Ⓕ  This paper was selected as Featured

View Online   Export Citation   CrossMark

**ARTICLES YOU MAY BE INTERESTED IN**

Thickness-scaling phonon resonance: A systematic study of hexagonal boron nitride from monolayers to bulk crystals
Journal of Applied Physics **132**, 134302 (2022); https://doi.org/10.1063/5.0094039

Photoexcited carrier dynamics in semi-insulating 4H-SiC by Raman spectroscopy
Journal of Applied Physics **132**, 135702 (2022); https://doi.org/10.1063/5.0108903

Process engineering of GaN power devices via selective-area p-type doping with ion implantation and ultra-high-pressure annealing
Journal of Applied Physics **132**, 130901 (2022); https://doi.org/10.1063/5.0107921

**APL Quantum**

**CALL FOR APPLICANTS**
Seeking Editor-in-Chief

# Mechanically tunable metasurface with large gamut of color: Lateral hybrid system Ⓕ

View Online    Export Citation    CrossMark

Rui Fang, Amir Ghasemi, ⓘD Dagou A. Zeze, ⓘD and Mehdi Keshavarz Hedayati[a) ⓘD

## AFFILIATIONS

Department of Engineering, Durham University, Durham, United Kingdom

[a)]Author to whom correspondence should be addressed: mehdi.keshavarz-hedayati@durham.ac.uk

## ABSTRACT

Hybrid metasurfaces are made of metals and dielectrics in which dielectrics (metals) are sandwiched between metals (dielectrics) to control the reflection and transmission of light. The existing designs have low sensitivity, little color coverage, and a lack of flexibility. Here, a new structural color design is proposed in which metals and dielectric resonators are arranged spatially in 2D to form a lateral hybrid system, instead of being placed as layers. Such a design exhibits a high level of sensitivity to mechanical forces because it works via 2D optical coupling and light confinement between adjacent resonators. Our study shows that in-planar coupling of two dissimilar resonators can enhance sensitivity by an order of magnitude in comparison to stacking them. Metasurfaces with our design would have unprecedented mechanical tunability without compromising either the materials choice or processing. Using the proposed hybrid system, we demonstrate large tunability across the full range of colors with only a 10% change in the size of the lattice, which further proves its superiority over existing designs. This concept could find application in wearable devices that require high sensitivity to small mechanical fluctuations.

## I. INTRODUCTION

Optical metasurfaces are subwavelength 2D structures with patterns that interact strongly with light, thus altering the light–matter interaction over subwavelength thickness. Artificially designed structures can fill in the gaps in the electromagnetic spectrum where materials are unable to respond, enabling the construction of new devices for applications, such as perfect absorbers,[1] anti-reflectors,[2] topological insulators,[3] digital-coding,[4] programmable metasurface,[5,6] information metamaterials,[7] flat lenses,[8] and structural color.[9,10] Their properties and functionalities are largely dictated by their spatial arrangement rather than intrinsic chemical properties. From the materials perspective, noble metals[11] and high refractive index dielectrics[12] have been used as the building blocks of metasurfaces due to their optical properties.

The coupling of the electromagnetic field between the adjacent resonators is the primary reason for using resonators in metasurfaces. In metallic nanoparticles (NPs), the free electron oscillation at the surface can couple with the proximal one, creating a bonding or anti-bonding hybridized mode, in analogy to the hybridization of atomic orbitals in molecules.[13] Although such hybridization (bonding mode, in particular) can create an intense field enhancement in the gap region, metals naturally suffer large parasitic losses. This increases significantly the probability of non-radiative photon recombination.[14] This inevitable problem stimulates the research on the high permittivity, low-loss dielectric counterpart, whose optical confinement can be achieved through the generation of intensive displacement current inside the structure, leading to either an electric dipole mode (ED) or a magnetic dipole mode (MD) depending on the wavelength.[14] However, low-loss dielectric dimers are limited by relatively weak optical confinement. A hybrid composed of both metal and dielectric can instead benefit from both worlds.

The field of metasurface structural color saw an increment in layering hybrid systems, i.e., dielectric resonator with metal cap,[15–17] sandwich structure,[18,19] nanoparticles on substrates,[20,21] nanocomposite,[22] multilayer[23,24] core-shell,[25] and grating.[26] Although the conventional hybrid designs show different levels of color tunability, real-time tuning (reversible) is out of reach because their tuning usually involves a change in material thickness, which is not possible post-processing. In some cases, flexible polymers or biodegradable materials[27] have been used as a substrate or a base; however, the tunabilities are very small and limited.[28–30]

In this paper, we present the first hybrid system in a planner arrangement by combining horizontally high permittivity dielectric and noble metals. As proof of concept, we demonstrate the application of the new design in structural color. The color tuning method in such a design relies on the change in the inter-resonator gap, which can be an advantage toward a flexible, stretchable metasurface. In this contribution, we have performed a comprehensive numerical investigation of the optical response of a lateral hybrid system. Different material pairs were studied with an altering lattice size.

## II. MATERIALS AND METHODS

Different system configurations are shown in Fig. 1. A typical mono-material metasurface is presented in Fig. 1(a), where all the resonators are composed of the same material. Figures 1(b) and 1(c) represent the lateral and layering system, respectively. Yellow and purple colors are used to differentiate materials. In the lateral system, resonators composed of two different materials are placed horizontally next to each other to form a lattice. In the layering system, one material is placed on top of the other as a shape of a cylinder resonator. The lattice size (P), pillar height (H), pillar diameter (D), and gap size (G) are also displayed in the graph. We select silicon (Si) and germanium (Ge) as dielectrics for their high refractive index and low loss in the visible region. Si has been of high interest for structural color since it is reliable, cost-effective, and easy to integrate into opto-electronic devices.[31] In contrast to other dielectric materials, for which the magnetic-type resonance is commonly dominant, Ge has a strong electric-type resonance due to its semi-metal properties, which can in theory create stronger coupling when placed next to a metal resonator.[32] Aluminum (Al) and gold (Au) are chosen as metal representatives due to their distinct features in dielectric functions in the visible region. Gold, although proven high loss in the visible wavelength, possesses better stability in most environments.[33,34] Al, on the other hand, has material properties that enable strong plasmon resonances spanning much of the visible region of the spectrum and into the ultraviolet. This extended response, combined with its natural abundance, low cost, and amenability to manufacturing processes, makes Al an auspicious material for commercial applications.[35,36]

## III. RESULTS

The three aforementioned systems have been built and the results are calculated by the commercially available software COMSOL Multiphysics. Figure 1(d) shows the schematic of a typical FEM model employed in the analysis. The simulated lattice is shown in Fig. 1(b), with a solid line square. Floquet periodic boundary conditions (PBCs) have been applied to the lateral faces (i.e., x and y directions) to mimic an infinite array of elements, and perfectly matched layers (PMLs) are placed at the top and bottom boundaries to avoid reflections from the ports. Floquet ports have been used to produce an x-polarized wave incident on the metasurface and monitor the reflected wave. The whole structure is meshed with triangular elements in the x and y directions. Meshing in the z direction is carried out by projecting elements from the x and y directions. The maximum mesh size is set to $\lambda_0/5$ in air and $\lambda_m/10$ in materials. A varying P, which increases from 150 to 200 nm, with a step of 25 nm, is adapted. All resonators have the same H

and D of 100 nm. This design led to a G size of 6.07 nm for P = 150 nm, 23.74 nm for P = 175 nm and 41.42 nm for P = 200 nm.

The result of mono-material systems at P = 150 nm is shown in Fig. 1(e). As expected, Si has demonstrated sound characteristics for color generating by a single, narrow peak, while Al, Ge, and Au showed relatively flat, low-intensity features. These results suggest that Si is more suited for color generation, thus the pairs of Si–Al, Si–Ge, and Si–Au should be taken to further investigation.

The Si–Al [Fig. 2(ai)] and Si–Ge [Fig. 2(bi)] lateral hybrid systems show a change in reflectance intensity and a blue shift of the reflectance dip around 525 nm with the increasing lattice size. Smaller gap size leads to stronger E field resonance, thus a higher reflectance intensity. It also allows stronger coupling between the E fields produced by both materials. The Si–Au pair has experienced a more dramatic change; two distinct peaks at $\lambda = 450$ nm and $\lambda = 540$ nm has merged into one as the lattice size enlarged [Fig. 2(ci)]. On the other hand, the layering hybrid system does not show any significant resonating frequency shifts. All three pairs see a unified change in the reflectance intensity. The color results of the lattice tuning of the two hybrid systems are shown in the CIE diagram in Fig. 2(iii). The lateral hybrid system is represented by the white/orange square and the layering hybrid is expressed by an array of white/blue squares. According to the color data, the lateral hybrid system shows a better color tuning range than its layering counterpart. The Si–Au pair, in particular, has exhibited the best color coverage, ranging from orange/yellow to the blue region.

The physics that governs the metal–dielectric lateral hybrid system has been studied with a simplified metal–dielectric dimer model.[16,37–43] Generally, the excited resonating mode from metal (plasmonic) and dielectric (Mie) is inherently different. Depending on their size and gap distance, different reflectance spectrums can be realized. In metal resonators, free electrons in metal interact with incident light, creating surface plasmon resonance (SPR).[11] When the diameter of the nanoresonator is small enough, the resonance is localized; hence, we have localized surface plasmon resonance (LSPR).[44] This type of resonance is mainly contributed by the ED and leaks more into the ambience.[41] It is, therefore, rather sensitive to environmental change such as inter-particle distance. For dielectric resonators, oscillating bond electrons create displacement currents when interacting with incident light, leading to Mie resonance.[12] In this type of resonance, the lower order of resonance such as MD and ED are most expressed, with the likelihood of a higher resonating mode (electric and magnetic quadrupole) when the size of the resonator increases.[32] With MD dominating the scattering field, it is less likely to be affected by the environment. A strong scattering field is usually achieved due to the low loss in dielectric resonators. The reflectance of a lateral system can then be viewed as the addition of that of mono-dielectric metasurface with an influence of the gap coupling between dielectric and metal resonators. For example, in Fig. 2(ci), the resonating peak at 450 nm is mainly contributed by the dielectric resonator. The shifting peak at 540 nm is contributed by the gap resonance of the Au resonator. This further demonstrates the ability to engineer the reflectance at will by carefully selecting the material combinations.

The electric and magnetic field intensity at $\lambda = 450$ nm and $\lambda = 540$ nm is shown in Fig. 3. A substantial electric field
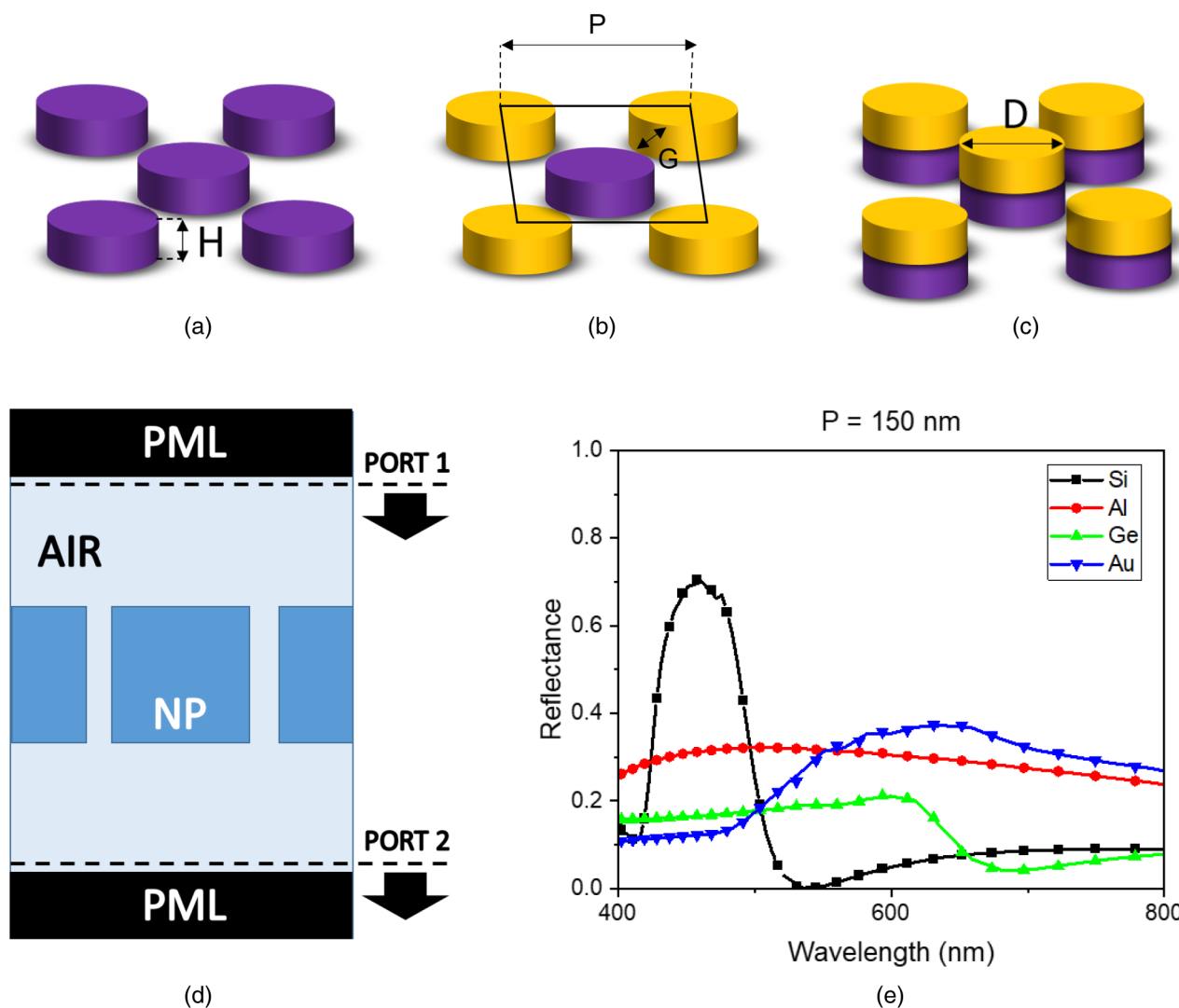
**FIG. 1.** Schematics of the designed mono- and hybrid systems. (a), (b), and (c) stand for mono-material system, lateral hybrid system, and layering hybrid system, respectively. The resonator diameter, height, gap between two resonators, and lattice size are indicated in the image. (d) demonstrates a single simulation unit in 2D, COMSOL. (e) shows the reflectance of mono-system with different materials at D = 100 nm, H = 100 nm, and P = 150 nm.

enhancement is observed in the gap region, indicating strong ED to ED coupling between metal and dielectric NPs. Meanwhile, a strong magnetic field enhancement is established inside the dielectric NP due to the presence of MD resonance, which also induces a certain magnetic field enhancement at the surface of the metal NP. This is due to the ED to MD coupling. At 450 nm, all three lattice size designs showed a high-intensity reflectance peak. The corresponding magnetic field intensity supports such a claim; the central Si resonator experienced intense scattering strength in all lattice sizes. On the other hand, a strong E field intensity at $\lambda = 450$ nm was only observed in a lattice size of 150 nm, which corresponds to

the peak at $\lambda = 540$ nm in the reflectance spectrum shown in Fig. 2 (ciii). Thus, we may conclude that the peak around 450 nm is achieved due to the intense MD generated by the dielectric part of the design, while the resonance peak at around 540 nm is due to the high ED scattering resulting from the metal part.

More interestingly, as the lattice size increases from 175 to 200 nm which corresponds to gap changes from 6.07 to 41.42 nm, little to no E field intensity or reflectance peak change is observed. This result agrees with previous studies, which suggest that the tuning effect is only present when the gap between metal and dielectric resonators is smaller than 20 nm.[37,42] Therefore, we
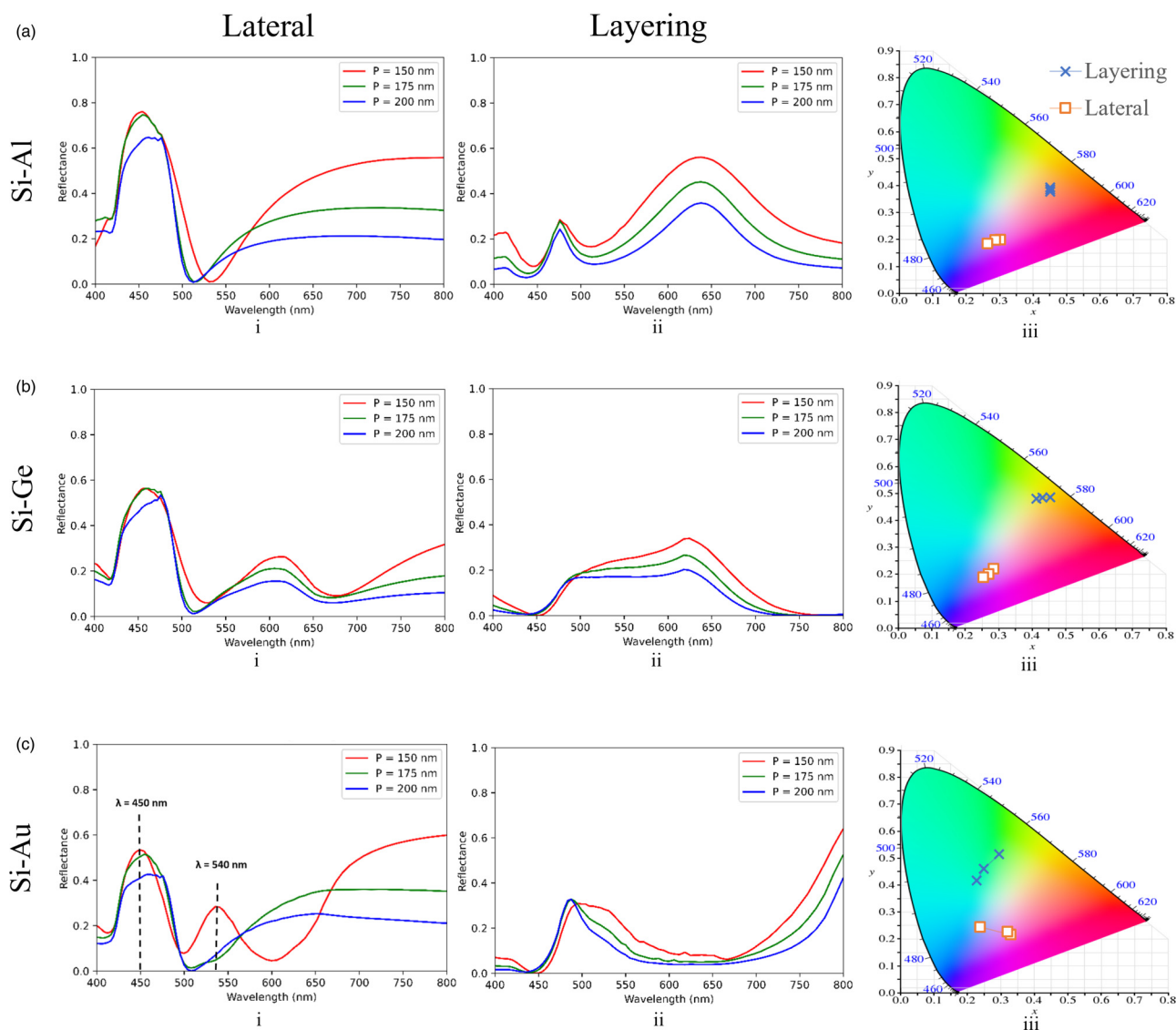
**FIG. 2.** Period tuning reflectance spectrum of different Si hybrid systems and their corresponding color. The reflectance of Si–Al, Si–Ge, and Si–Au is presented in (a), (b), and (c), respectively. (i) shows the lateral hybrid [Fig. 1(b)], and (ii) represents the layering hybrid system [Fig. 1(c)]. (iii) shows the CIE color map of Si–Al, Si–Ge, and Si–Au lateral and layering system lattice tuning accordingly.

designed a smaller range of lattice tuning to investigate the color tuning effect further.

When the metal and dielectric NPs are brought into close proximity, the coupling between the metal LSPR and dielectric Mie resonances modifies the optical response of the entire structure.[14] The primary ED and MD moment excited by incident light could induce a secondary ED and MD moment on the other part, which would, in turn, alter both the amplitudes and phases of the electric and magnetic dipolar resonances of the dimer and largely modify its scattering properties.[14] Furthermore, when placed nearby the

ED generated by both materials would create two new modes, bonding and anti-bonding modes. A bonding mode occurs when the electric fields in both resonators are circulating in the same direction (i.e., both clockwise), whereas an anti-bonding mode emerges when the electric fields are circulating in the opposite direction (one clockwise and the other anti-clockwise).[45]

We further investigate the Si–Au pair by a small lattice size ranging from 145 to 175 nm. This design allows the gap size to increase linearly from 2.53 to 23.74 nm. The effect of these two modes on the reflectance is shown in Fig. 4. Significant dips can be
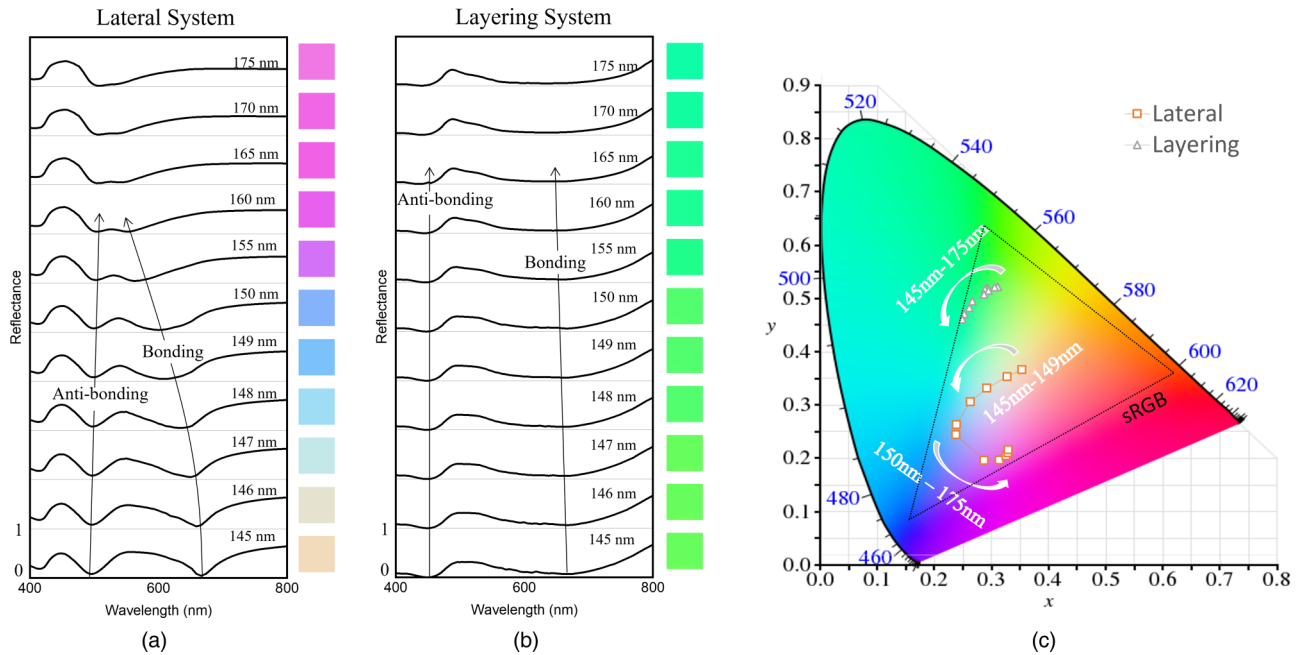
**FIG. 3.** Field intensity of Si–Au lateral hybrid system. The lattice size ranged from 150 to 200 nm, with a 25 nm step. Electric and magnetic field intensity at $\lambda = 450$ nm and $\lambda = 540$ nm are presented.

observed where the bonding and anti-bonding modes appeared. As the lattice size increases, the bonding mode in the lateral has shifted drastically from around 665 nm to around 520 nm [Fig. 4(a)], while in the conventional hybrid design, both bonding and anti-bonding resonating wavelengths reveal very limited change [Fig. 4(b)]. This observation proves that the bonding mode is more sensitive to the gap size, giving opportunities to tune the reflected color based on a lattice tuning method.

The reflected colors and the standard sRGB area are shown in Fig. 4(c). We observe a well-covered color range from orange/yellow to, blue, violet, and pink, then finally terminated in the red-violet region. The color coverage has reached 14% of the sRGB color map, whereas the bare color of green and a less than 1% coverage have been found in the layering system. The coverage is obtained by quantitatively comparing the color gamut with the sRGB standard spaces via calculating the area.

A comparison of lattice tuning of our lateral design and conventional hybrid layering designs,[17,23,24] which are reported in the literature, is shown in Fig. 5. In this figure, "25%–75%" demonstrates that from low to high, 25%–75% of data fall into this range. Similarly, "10%–90%" demonstrates that 10%–90% of data fall into this range, and "Mean" stands for the mean value for the data. We consider the sensitivity of the designed metasurface by the change in the resonating wavelength over the change in the lattice size ($\Delta\lambda/\Delta p$). The change in the lattice size would mimic a mechanically stretchable metasurface, thus proving the sensitivity to mechanical forces. The lateral design clearly has a higher influencing parameter ranging from 3 to 26, with a mean value of 11. On the other hand, the layering systems only showed little effect with a

factor of around 2 or lower. In other words, the hybrid lateral system sensitivity is ten times the conventional metasurfaces. This further highlights the performance of the proposed lateral hybrid system to a conventional layer system. Furthermore, the existing
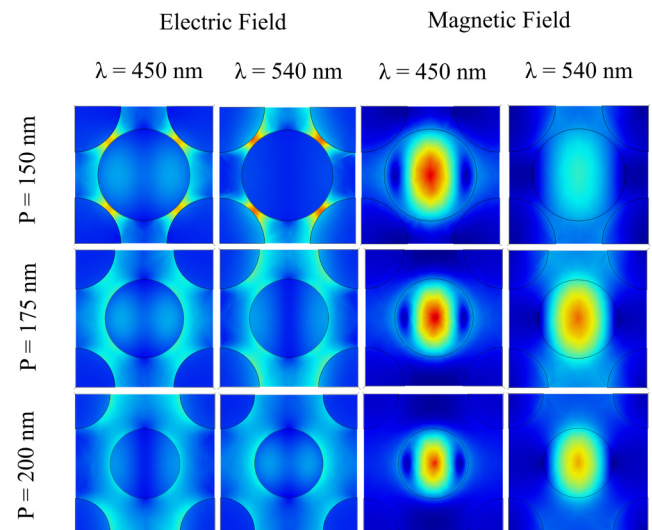


**FIG. 4.** Results of lattice tuning from 145 to 175 nm of Si–Au hybrid systems. (a) and (b) show the reflectance of lateral and layering systems accordingly. The color generated by the reflectance is extracted and shown next to each spectrum line. Their tuning color in the standard CIE system is presented in (c).
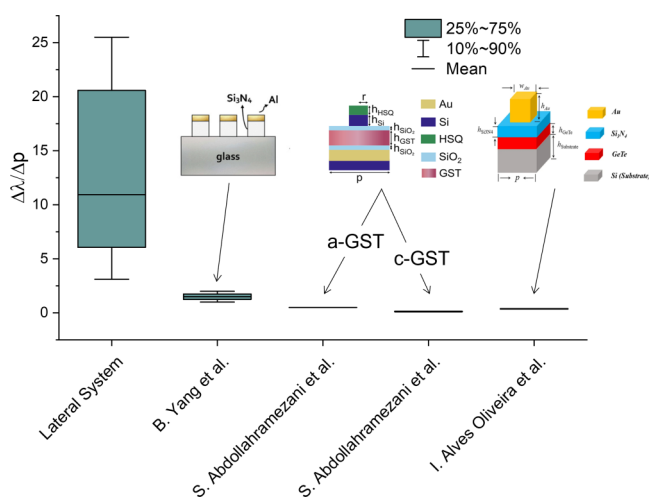
**FIG. 5.** Layering designs from past research and their tuning ability ($\Delta\lambda/\Delta p$), in comparison with our study. Figures reproduced with permission from Yang *et al.*, Adv. Opt. Mater. **9**(21), 2100895 (2021). Copyright 2021 John Wiley and Sons; Abdollahramezani *et al.*, Nano Lett. **21**(3), 1238 (2021). Copyright 2021 American Chemical Society; Alves Oliveira *et al.*, Sci. Rep. **11**(1), 21919 (2021). Copyright 2021 Author(s), licensed under a Creative Commons Attribution (CC BY) license.

"period" tuning layering systems have a rather fixed feature. To the best of our knowledge, the lattice tuning effects are based on many rigid (already fabricated) metasurfaces with different lattice sizes. The superiority of the lateral system lies in its ability to adapt to a flexible and stretchable substrate.

This tuning effect could potentially be adapted to other metal–dielectric pairs with various parameters. There are various choices in metals (e.g., Al, Ag, Au, Cu) and dielectric materials with intermediate or high refractive indexes (e.g., ITO, GaP, Si, Ge, GaAs). The numerous combination possibilities among them provide a large degree of freedom to tune the optical response of the heterodimer, covering, therefore, a broad color range. Future work can be considered in terms of the surface profile to realize higher quality colors.

## IV. CONCLUSIONS

Here, we present a metal–dielectric hybrid system in a planner configuration. According to the range of materials examined in this study, the Si–Au pair exhibits the highest sensitivity and color coverage. It turned out that the hybrid planner system is not only more flexible and stretchable but also ten times more sensitive than its layering counterpart. The flexibility in processing provided by the proposed approach may make real-time tunable mechanical metasurfaces possible. Given the large gamut of color, the new metasurface could be used as a broadband detector for tactile and vibration sensors, which is otherwise not possible with conventional metasurfaces.

## ACKNOWLEDGMENTS

## AUTHOR DECLARATIONS

### Conflict of Interest

The authors have no conflicts to disclose.

### Author Contributions

**Rui Fang:** Conceptualization (equal); Data curation (lead); Formal analysis (lead); Investigation (equal); Methodology (equal); Writing – original draft (lead); Writing – review & editing (equal). **Amir Ghasemi:** Formal analysis (equal); Methodology (equal); Writing – review & editing (equal). **Dagou A. Zeze:** Conceptualization (equal); Investigation (equal); Supervision (equal); Writing – review & editing (equal). **Mehdi Keshavarz Hedayati:** Conceptualization (lead); Funding acquisition (lead); Investigation (equal); Methodology (equal); Supervision (lead); Writing – review & editing (lead).

## DATA AVAILABILITY

The data that support the findings of this study are available from the corresponding author upon reasonable request.

## REFERENCES

[1]Y. Yao, R. Shankar, M. A. Kats, Y. Song, J. Kong, M. Loncar, and F. Capasso, Nano Lett. **14**, 6526 (2014).
[2]M. Keshavarz Hedayati, M. Abdelaziz, C. Etrich, S. Homaeigohar, C. Rockstuhl, and M. Elbahri, Materials **9**, 636 (2016).
[3]J. W. You, Q. Ma, Z. Lan, Q. Xiao, N. C. Panoiu, and T. J. Cui, Nat. Commun. **12**, 1 (2021).
[4]C. Liu, Q. Ma, Z. J. Luo, Q. R. Hong, Q. Xiao, H. C. Zhang, L. Miao, W. M. Yu, Q. Cheng, and L. Li, Nat. Electron. **5**, 113 (2022).
[5]Q. Ma, G. D. Bai, H. B. Jing, C. Yang, L. Li, and T. J. Cui, Light Sci. Appl. **8**, 1 (2019).
[6]L. Chen, Q. Ma, Q. F. Nie, Q. R. Hong, H. Y. Cui, Y. Ruan, and T. J. Cui, Photonics Res. **9**, 116 (2021).
[7]Q. Ma and T. J. Cui, PhotoniX **1**, 1 (2020).
[8]S. Wang, P. C. Wu, V.-C. Su, Y.-C. Lai, M.-K. Chen, H. Y. Kuo, B. H. Chen, Y. H. Chen, T.-T. Huang, J.-H. Wang, R.-M. Lin, C.-H. Kuan, T. Li, Z. Wang, S. Zhu, and D. P. Tsai, Nat. Nanotechnol. **13**, 227 (2018).
[9]N. B. Roberts and M. Keshavarz Hedayati, Appl. Phys. Lett. **119**, 061101 (2021).
[10]X. Zhu, J. Engelberg, S. Remennik, B. Zhou, J. N. Pedersen, P. Uhd Jepsen, U. Levy, and A. Kristensen, Nano Lett. **22**, 2786 (2022).
[11]M. Keshavarz Hedayati and M. Elbahri, Plasmonics **12**, 1463 (2017).
[12]K. Baek, Y. Kim, S. Mohd-Noor, and J. K. Hyun, ACS Appl. Mater. Interfaces **12**, 5300 (2020).
[13]P. K. Jain and M. A. El-Sayed, Chem. Phys. Lett. **487**, 153 (2010).
[14]S. Kim, J. Jin, Y.-J. Kim, I.-Y. Park, Y. Kim, and S.-W. Kim, Nature **453**, 757 (2008).
[15]K. Kumar, H. Duan, R. S. Hegde, S. C. W. Koh, J. N. Wei, and J. K. W. Yang, Nat. Nanotechnol. **7**, 557 (2012).
[16]D. Ray, T. V. Raziman, C. Santschi, D. Etezadi, H. Altug, and O. J. F. Martin, Nano Lett. **20**, 8752 (2020).
[17]B. Yang, W. Liu, D. Choi, Z. Li, H. Cheng, J. Tian, and S. Chen, Adv. Opt. Mater. **9**, 2100895 (2021).
[18]B. Fang, C. Yang, W. Shen, X. Zhang, Y. Zhang, and X. Liu, Appl. Opt. **56**, C175 (2017).
[19]Z. He, W. Xue, W. Cui, C. Li, Z. Li, L. Pu, J. Feng, X. Xiao, X. Wang, and G. Li, Nanomaterials **10**, 687 (2020).

[20]F. Todisco, R. Malureanu, C. Wolff, P. Gonçalves, A. S. Roberts, N. A. Mortensen, and C. Tserkezis, Nanophotonics **9**, 803 (2020).

[21]A. Assadillayev, T. Hinamoto, M. Fujii, H. Sugimoto, M. L. Brongersma, and S. Raza, ACS Photonics **8**, 1582 (2021).

[22]M. K. Hedayati, S. Fahr, C. Etrich, F. Faupel, C. Rockstuhl, and M. Elbahri, Nanoscale **6**, 6037 (2014).

[23]S. Abdollahramezani, O. Hemmatyar, M. Taghinejad, H. Taghinejad, Y. Kiarashinejad, M. Zandehshahvar, T. Fan, S. Deshmukh, A. A. Eftekhar, W. Cai, E. Pop, M. A. El-Sayed, and A. Adibi, Nano Lett. **21**, 1238 (2021).

[24]I. Alves Oliveira, I. L. Gomes De Souza, and V. F. Rodriguez-Esquerre, Sci. Rep. **11**, 21919 (2021).

[25]A. Sheverdin and C. Valagiannopoulos, Phys. Rev. B **99**, 075305 (2019).

[26]A. De Proft, K. Lodewijks, B. Figeys, D. Kouznetsov, N. Verellen, N. P. Pham, B. Vereecke, D. Sabuncuoglu Tezcan, R. Jansen, P. Van Dorpe, and X. Rottenberg, ACS Photonics **9**, 1349 (2022).

[27]V. Caligiuri, G. Tedeschi, M. Palei, M. Miscuglio, B. Martin-Garcia, S. Guzman-Puyol, M. K. Hedayati, A. Kristensen, A. Athanassiou, R. Cingolani, V. J. Sorger, M. Salerno, F. Bonaccorso, R. Krahne, and J. A. Heredia-Guerrero, ACS Nano **14**, 9502 (2020).

[28]W. Niu, K. Zhao, L. Qu, and S. Zhang, J. Mater. Chem. C **6**, 8385 (2018).

[29]G. Zhang, W. Peng, J. Wu, Q. Zhao, and T. Xie, Nat. Commun. **9**, 1 (2018).

[30]W. Zhang, H. Wang, H. Wang, J. Y. E. Chan, H. Liu, B. Zhang, Y.-F. Zhang, K. Agarwal, X. Yang, A. S. Ranganath, H. Y. Low, Q. Ge, and J. K. W. Yang, Nat. Commun. **12**, 1 (2021).

[31]A. Leitis, A. Heßler, S. Wahl, M. Wuttig, T. Taubner, A. Tittl, and H. Altug, Adv. Funct. Mater. **30**, 1910259 (2020).

[32]P. D. Terekhov, K. V. Baryshnikova, Y. A. Artemyev, A. Karabchevsky, A. S. Shalin, and A. B. Evlyukhin, Phys. Rev. B **96**, 035443 (2017).

[33]S. K. Balasubramanian, L. Yang, L.-Y. L. Yung, C.-N. Ong, W.-Y. Ong, and L. E. Yu, Biomaterials **31**, 9023 (2010).

[34]G. V. Naik, V. M. Shalaev, and A. Boltasseva, Adv. Mater. **25**, 3264 (2013).

[35]M. W. Knight, N. S. King, L. Liu, H. O. Everitt, P. Nordlander, and N. J. Halas, ACS Nano **8**, 834 (2014).

[36]R. L. Olmon, B. Slovick, T. W. Johnson, D. Shelton, S.-H. Oh, G. D. Boreman, and M. B. Raschke, Phys. Rev. B **86**, 235147 (2012).

[37]A. Barreda, S. Hell, M. A. Weissflog, A. Minovich, T. Pertsch, and I. Staude, J. Quant. Spectrosc. Radiat. Transfer **276**, 107900 (2021).

[38]P. Nordlander, C. Oubre, E. Prodan, K. Li, and M. I. Stockman, Nano Lett. **4**, 899 (2004).

[39]I. Romero, J. Aizpurua, G. W. Bryant, and F. J. García De Abajo, Opt. Express **14**, 9988 (2006).

[40]J. Shi, L. Ju, X. Zhang, Y. Huang, and Y. Fang, Spectrochim. Acta, Part A **266**, 120465 (2022).

[41]S. Sun, M. Li, Q. Du, C. E. Png, and P. Bai, J. Phys. Chem. C **121**, 12871 (2017).

[42]S. Sun, D. Wang, Z. Feng, and W. Tan, Nanoscale **12**, 22289 (2020).

[43]Q. Zhao, Z.-J. Yang, and J. He, Front. Phys. **13**, 1 (2018).

[44]M. Song, D. Wang, S. Peana, S. Choudhury, P. Nyga, Z. A. Kudyshev, H. Yu, A. Boltasseva, V. M. Shalaev, and A. V. Kildishev, Appl. Phys. Rev. **6**, 041308 (2019).

[45]E. Prodan, C. Radloff, N. J. Halas, and P. Nordlander, Science **302**, 419 (2003).